



ELSEVIER

Available online at [www.sciencedirect.com](http://www.sciencedirect.com)

SCIENCE @ DIRECT®

International Communications in Heat and Mass Transfer 32 (2005) 360–370

International Communications in  
**HEAT and MASS  
TRANSFER**

[www.elsevier.com/locate/ichmt](http://www.elsevier.com/locate/ichmt)

## Observation of preferred instability modes in a mechanically excited thermal plume using Schlieren visualizations<sup>☆</sup>

J.C. Elicer-Cortés<sup>a,\*</sup>, C. Ruz<sup>a</sup>, R.H. Hernández<sup>a</sup>, M. Pavageau<sup>b</sup>, D. Boyer<sup>c</sup>

<sup>a</sup>Universidad de Chile, Departamento de Ingeniería Mecánica, Beauchef 850, 5° Piso, Casilla 2777, Santiago, Chile

<sup>b</sup>Ecole des Mines de Nantes, GEPEA, UMR, CNRS 6144, 4, rue Alfred Kastler, B.P. 2072246, F-44307 Nantes Cedex 3, France

<sup>c</sup>Universidad Nacional Autónoma de México, Instituto de Física, Apartado Postal 20-364, 01000 México D.F., México

Available online 21 January 2005

### Abstract

An experimental study of the instability modes of a laminar axisymmetric thermal plume under symmetrical controlled disturbances of varicose type was carried out. The Schlieren technique was used to investigate the considered flow. The range of excitation frequencies over which the studied plume became unstable was determined. The size of the corresponding induced large-scale structures was analyzed in function of the disturbance frequency. The results obtained throughout this work confirmed the ability of a plume to behave like a frequencies filter.

© 2004 Elsevier Ltd. All rights reserved.

*Keywords:* Thermal plume; Mechanical forcing; Flow instabilities; Schlieren visualization

### 1. Introduction

In this paper, the emphasis is put on heated flows for which buoyancy forms the main source of fluid motion. Such flows are highly unstable. Their sensitivity to even slight disturbances (natural or imposed) is such that initially laminar regimes almost always become turbulent rather quickly.

The question of how and when buoyancy-driven flows become turbulent is an important matter from the applicative point of view. This has been illustrated by Cetegen et al. [1]. Turbulence will generally be

<sup>☆</sup> Communicated by J.P. Hartnett and W.J. Minkowycz.

\* Corresponding author.

*E-mail address:* [jelicer@cec.uchile.cl](mailto:jelicer@cec.uchile.cl) (J.C. Elicer-Cortés).

fostered any time high mixing efficiency is sought for. More interesting, perhaps, is that initially laminar flows may react differently to disturbances of different frequencies: a given disturbance may be damped or amplified so that turbulence may develop or not, at more or less fast rates. Consequently, a better knowledge of the preferential modes of a given flow may make it possible ultimately to design control systems able to trigger or inhibit the growth of turbulence depending on the targeted application. In other cases, it may merely be useful to be able to tune the pulsing, puffing, or flapping frequency of a flow to a desired frequency, or to look for the development of structures of specified scales. For example, in an axisymmetric plume rising from a flame, the periodic engulfment of air produced by the large-scale toroidal vortex rings forming close to the source is responsible for most of the plume entrainment. These vortices generate a periodic pumping whose magnitude is directly related to their circulation (Cetegen [2]). The model derived by Cetegen subsequently to his analysis provided a sounder foundation for the scaling of entrainment rates in the near field of fire plumes, which is of great interest with respect to fire safety science and engineering although incidental fires are not totally controllable flows.

The fate of a given disturbance in a given flow is not an easy matter. Basically, a disturbance evolves according to the net amount of energy input into it as it progresses downstream. The unstable behavior of a flow can be local or global, depending on whether a disturbance, initially located in space and time, will invade the whole flow or remain confined in a finite volume while it is transported by the mean flow.

Stability loss in thermal plumes pertains to a broader class of problems namely stability analysis of open systems (jets, wakes). The primary mechanism that makes initially laminar flows become turbulent is the initial growth of very small disturbances. The study of these instabilities is commonly approached by means of linear analysis. The approach consists in considering the effect of small departures from the equilibrium state by imposing velocity and/or temperature usually periodic disturbances much smaller than the velocity and/or temperature spatial variations within the developing laminar flow. Subsequently, only first-order terms are retained in the disturbed transport equations. This approximation along with others leads to considerable simplifications in the problem analysis. It is explained in a rather clear way by Gebhart et al. [3]. From this, it has been found that a frequent mechanism of disturbance growth in buoyancy-induced flows is a propagating downstream periodic wave alike the Tollmien–Schlichting wave observed in forced boundary layer flows. If the flow and buoyancy forces are able to continuously supply energy to these waves, the disturbance will grow in amplitude. Now, the process is selective so that the amplification or damping of a periodic wave depends on its frequency. Moreover, it is location dependent. Generally speaking, it has been observed that disturbances grow more quickly in free-boundary flows like heated plumes. The explanation is presumably the absence of solid surfaces to damp disturbances. Finally, when the amplitude of disturbances grows beyond the validity domain of the small disturbance approximation, non-linear growth mechanisms appear that generate higher harmonics and secondary flows.

Several studies have allowed establishing certain characteristics of instability phenomena for two-dimensional flows. Pera and Gebhart [4] introduced small symmetrical and asymmetrical perturbations in two-dimensional heated air plumes. They observed that high frequency disturbances did not affect the stability of the studied plumes. In a plane plume, Bill and Gebhart [5] observed that transition to turbulence occurred simultaneously for both the temperature and velocity fields, that temperature and velocity disturbances were permanently coupled with each other and that disturbances were amplified in a frequency-selective fashion.

It is interesting to note that the wavelength or the frequency of the waves developing in a plume (or in a jet) is usually well correlated with the characteristic dimensions of the studied flow and/or with

the characteristics of the disturbance source. Kimura and Bejan [6] noticed that during transition, the wavelength of the developing undulations at an axisymmetric plume boundary was well correlated to the local plume diameter. Cetegen [7] experimentally studied the effects of external disturbances on the behavior of axisymmetric helium and air-helium plumes. He observed that the immediate response of the plumes to imposed periodical disturbances was the regular formation of toroidal vortices at a frequency equal to the excitation frequency. These large-scale structures had dimensions of the order of the source diameter. Additionally, the main flow field appeared not to be influenced by the forcing frequency as long as this frequency was not too close from the natural frequency of the flow. Later on, Cetegen et al. [1] performed similar experiments for planar buoyant plumes of air-helium mixtures. The onset of pulsations within a height of a few nozzle widths from the source could be best correlated in terms of the plume source Reynolds number and the ratio of the initial mixture density to that of the ambient fluid. The oscillation frequency of the investigated plume configurations appeared to correlate well in terms of the Strouhal number  $St=fw/U_0$  and the Richardson number  $Ri$  yielding a correlation  $St=0.55Ri^{0.45}(1<Ri<10^2)$ .

In this paper, we present an experimental study of an initially laminar axisymmetrical plume subjected to controlled periodical and axisymmetrical disturbances (varicose mode). Measurements were performed in a non-intrusive way by using the Schlieren technique. The potential benefit of this technique was investigated for several configurations whereby the source temperature and the excitation frequency of the disturbance imposed on the flow were varied. In the following, some aspects of the technique are recalled briefly. We then describe the experimental apparatus used in the present study. This is followed by the presentation and discussion of the results regarding the preferred modes of the investigated plumes. We conclude this paper with a summary of the findings from this study.

## 2. Schlieren technique and experimental setup

The arrangement used in this work was of “Z” type in reference to the shape of the path followed by light. The main optical parts were a 25-W light source, two identical concave mirrors (f/10) 6 in. in diameter, a knife-edge (spatial filter), and a CCD video camera (Fig. 1). As they travel through the test flow region, the light beams are slightly bent owing to spatial variations of the refraction index with local density/temperature gradients within the flow. The contrasted image that finally forms on the screen downstream of the knife-edge exhibits clear and dark zones that allow flow visualization. Tanda [8] has successfully used this technique for the analysis of heat transfer by convection in different configurations. The reader is also referred to Settles [9] for a compilation of works showing a wide variety of applications in which the Schlieren technique was used, and for construction and operation advice.

Optical rails and appropriate stands were used to ensure an accurate alignment of the optical elements, to match focal lengths, and to adjust light path between the optical elements. The experimental arrangement was such that the height of the flow observation region could be varied easily while preserving the optical setup. To minimize astigmatism, chromatic aberration, and other optical effects inherent to the system, the angle of incidence of the light beams on the mirrors was set close to  $3^\circ$  [8]. A paper-diamond screen was placed between the knife-edge and the video camera. The Handy Cam camera used here was connected to a computer for image acquisition. The CCD array of the camera had a resolution of 320,000 pixels. The focal length of the objective was 3.6 to 72 mm.

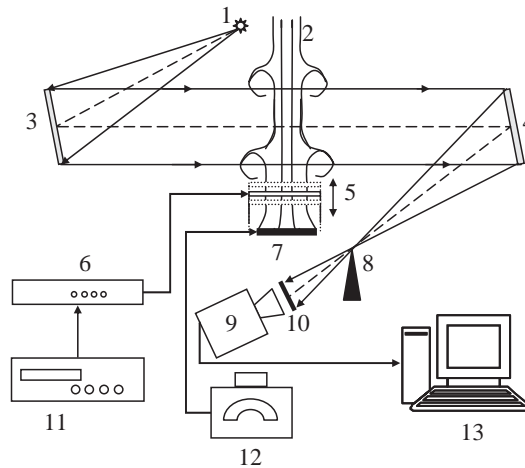


Fig. 1. Schematic representation of the experimental arrangement: (1) Light source; (2) Thermal plume; (3) Mirror #1; (4) Mirror #2; (5) Excitation apparatus; (6) Power amplifier; (7) Heat source; (8) Knife-edge; (9) CCD video camera; (10) Diamond-paper screen; (11) Function generator; (12) AC Power supply Variac; (13) PC Pentium IV with video acquisition board card.

Variations of the refraction index  $n$ , when  $n \approx 1$ , are given by the Gladstone–Dale equation in which  $C$  is the Gladstone–Dale constant, and  $\rho$  the fluid density:

$$\rho = \frac{n - 1}{C} \tag{1}$$

Assuming that the pressure is constant within the illuminated region, assuming also that the considered medium obeys the ideal gas state law, from geometrical considerations on the deflection angle of the light beams traversing the test region it is possible to relate the contrast of the image that forms on the end screen to the temperature gradient within the investigated flow region by means of an expression of the form:

$$\text{Contrast} \propto \pm \int -\frac{C\rho}{T} \frac{\partial T}{\partial x} dy \tag{2}$$

Eq. (2) states that the resulting contrast is proportional to the cumulative effect in the direction of the light beam (in the  $y$ -direction in the present case) of the temperature gradient in the direction normal to the section plane ( $x$ -direction here).

Details regarding the experimental setup have been given by Elicer-Cortés et al. [10] so that we shall here restrict ourselves to the essential aspects of it only. The apparatus consisted of a thermal source immersed into quiescent air at atmospheric pressure inside a  $2.0 \times 2.0 \text{ m}^2$  square base and 2.5-m high anechoic enclosure with double glazed walls. The investigated axisymmetric thermal plume was generated by an 8-mm-thick round metallic disk of diameter  $D=80 \text{ mm}$ . The disk could be heated electrically up to  $800 \text{ }^\circ\text{C}$  by a regulated AC power supply of 1 kVA. It allowed us to achieve turbulent flow regimes if desired. A thermocouple (K type) located only 0.3 mm below the active surface allowed accurate measurements of the temperature at the disk surface. Great care was exercised in the design and construction of the present arrangement so that it allowed the generation of almost ideal thermal plumes in an “infinite” adiabatic ambient fluid at rest without any temperature stratification.

The flow was excited mechanically by means of an oscillating toroidal metal ring with an outer diameter of 93 mm located at the periphery of the heat source, slightly downstream of it so as to appropriately disturb the initial plume entrainment. The disturbance generated this way was of varicose type. The downstream position of the ring with respect to the hot disk surface was adjustable. This allowed us to investigate various flow regions. Sinusoidal signals from a function generator TK-AFG-320 were applied to a speaker after amplification by a potential amplifier model type NF-HSA-4011. The periodic movement of the 15-cm diameter central part of the speaker was then transmitted to the ring by means of 3 thin rods 2 mm in diameter. The maximum amplitude of the movement of the ring was 8 mm approximately. Great care was exercised to perfectly align the ring axis with the source axis so that the disturbance generated this way was fully symmetrical. The cross-section of the toroidal ring was only 5 mm in diameter in order to prevent the shedding of Von Kármán type vortices in the entrained airflow ( $Re < 50$ ). Wake vortices were avoided in the vicinity of the source so as not to generate additional disturbances that could have led to misinterpretations of the results. Finally, a circular deflector was provided between the loudspeaker and the heat source to suppress any potential influence of the air volume displaced by the movement of the loudspeaker (air pumping).

### 3. Methodology

The circular observation window was centered at a height  $z_C = 15$  cm ( $z_C/D = 1.88$ ) above the heat source. Since the mirrors were 6" in diameter (15.24 cm), the lower and upper limits of the observation window corresponded to  $z = 7$  cm and  $z = 22$  cm, respectively. Tests were also performed for  $z_C = 21$  cm. However, the structures we could observe had too fuzzy contours to make the results interpretable.

As the controlled disturbances had to be applied to an initially laminar and stable thermal plume, the first visualizations were made to check for the flow laminarity and stability dependency on the source temperature. It was observed that the flow remained laminar in the test region up to a source temperature of 200 °C (see Fig. 2). Consequently, the experiments were carried out for 3 source temperatures namely 100 °C, 150 °C, and 200 °C.

The experimental protocol was as follows: the voltage of the AC Variac power supply was adjusted until the desired source temperature was reached and had stabilized. Controlled disturbances were

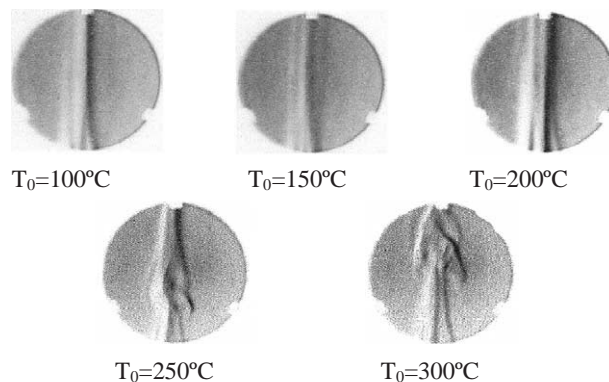


Fig. 2. Influence of temperature on the stability of the thermal plume.

applied to the flow so as to determine roughly the excitation frequency range over which the flow reacted by developing vortex rings. The whole frequency range was scanned again with a frequency step of 0.5 Hz or 0.1 Hz over the range where the flow reaction was most remarkable. For each disturbance frequency, the flow was filmed during 5 s at a frame rate (FR) of 20 frames per second. The acquired images were then processed using a program routine made in Matlab to derive the characteristic dimensions of the observed structures.

In first approximation, the mean advection velocity  $U_a$  of the structures at a given excitation frequency was estimated by considering the number of frames  $N$  necessary for a structure to cross the entire observation domain vertically (mirrors diameter, 6" or 0.15 m) and the acquisition frame rate FR of the video camera. It was then inferred:

$$U_a = \frac{\text{FR}}{N} 0.15 \text{ m/s} \quad (3)$$

Although the mean advection velocity varied slightly with the disturbance frequency, a single average advection velocity was considered for each investigated source temperature.

#### 4. Discussion of results

The development of vortex rings (toroidal structures) of varicose mode was observed for excitation frequencies between  $f=1$  Hz and  $f=9$  Hz for the source temperature range considered here. The flow did not react to higher disturbance frequencies. This is in good agreement with earlier results obtained by other measurement techniques [4–6].

Fig. 3 shows a typical plume behavior for a source temperature of 150 °C and for  $z_c/D=1.88$  (see also Fig. 4 for a source temperature of 200 °C). Structures of highest amplitude were obtained for  $f$  about 2.2 Hz in this particular case. This frequency was called the natural frequency or the preferential mode of the flow. It corresponds to a situation of resonance. The corresponding Strouhal number based on an estimated mean advection velocity  $U_a=0.28$  m/s of the structures was about  $St=0.63$ . Note that Han and Goldstein [11], who investigated the response of slightly heated free jets subjected to acoustic disturbances, found that the frequency associated with the passage of the observed vortices was characterized by Strouhal numbers  $St \approx 0.65$  at  $z/D=1$  and  $St \approx 0.40$  for  $z/D=4$ . Although these Strouhal numbers are not based on the same frequency scale as our, it is interesting to note how both definitions give results that coincide rather well.

Qualitatively similar behaviors were observed for the three work temperatures. For example, Fig. 4 shows the behavior of the flow subjected to excitation frequencies ranging from  $f=0$  Hz to  $f=8$  Hz, for a

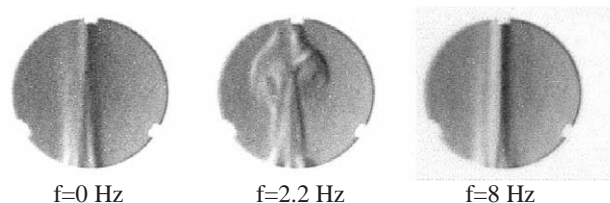


Fig. 3. Limits of instability of the thermal plume,  $T_0=150$  °C.

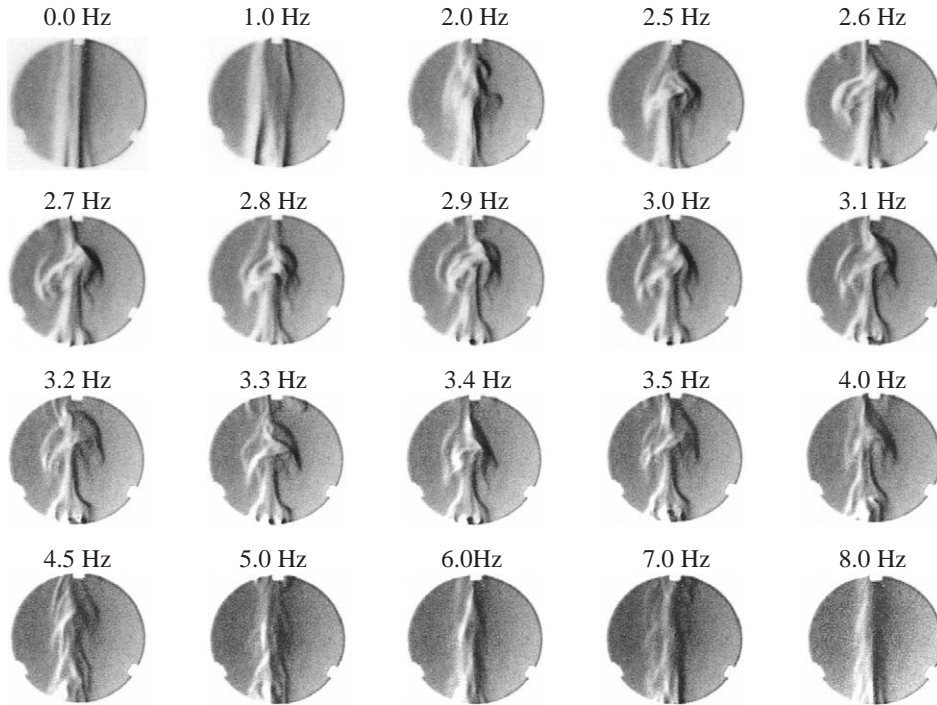


Fig. 4. Flow structure changes with increasing disturbance frequency,  $T_0=200\text{ }^\circ\text{C}$ .

heat source temperature of  $200\text{ }^\circ\text{C}$ . As already stated, no structure is present for  $f < 1\text{ Hz}$  and  $f > 9\text{ Hz}$ . It can be noticed that the structures grow in size with increasing the excitation frequency, reach a maximum diameter, and then shrink until the flow comes back to a stable state ( $f > 9\text{ Hz}$ ). It was observed that the larger structures appeared at excitation frequencies between  $1.5\text{ Hz}$  and  $3.0\text{ Hz}$  depending on the temperature of the heat source.

It was also observed that structures form with a certain regularity. For example, the same pattern can be observed in frames #3, #9, and #15 of Fig. 5. The corresponding repetition rate matches the excitation frequency almost exactly. Actually, as the excitation frequency was  $3.2\text{ Hz}$  in this particular case, an exact match would have entailed identical images every 6.25 frames. Since the image acquisition rate used here is not an exact multiple of the imposed excitation frequency, the match cannot be exact.

Some topological features of the observed structures were inferred from the acquired images and by means of a program routine in Matlab. Relevant notations are given in Fig. 6. The diameter  $D_m$  of the mirrors was taken as reference length. The dimensions of the left-hand side and the right-hand side cross-sections of the same toroidal structure were distinguished. Note that the initially circular cross-section of the toroidal structures often become ellipsoidal with dimensions  $2a$  and  $2b$  as they are convected by the mean flow owing to stretching by shear stress and buoyancy forces (subscripts  $l$  and  $r$  denote left and right sides, respectively). By analogy to the definition of the hydraulic diameter, an equivalent structure diameter  $D_e$  was defined as:

$$D_e = \frac{4 \text{ Area of the ellipsoidal section}}{\text{Wet perimeter}} = \frac{ab}{\sqrt{\frac{1}{8}(a^2 + b^2)}} \tag{4}$$

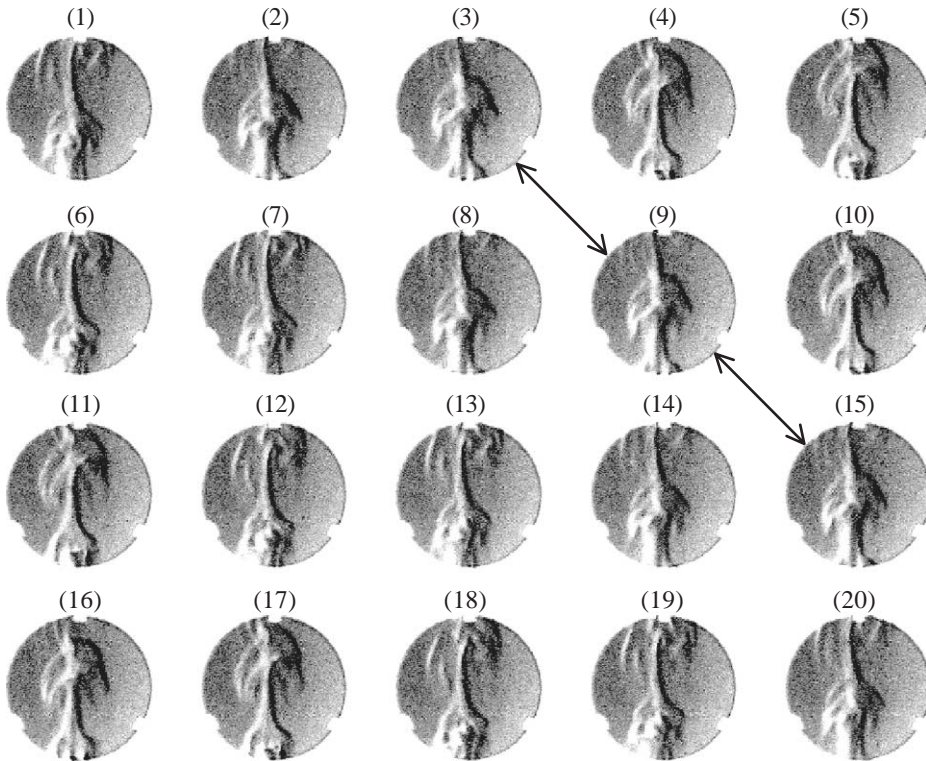


Fig. 5. Sequence of images for:  $t=1.0$  s;  $f=3.2$  Hz;  $T_0=200$  °C.

In the analysis, we will use  $D_S$  with  $D_S=(D_{e,l}+D_{e,r})/2$ . We also define:  $S$ , the distance between the centers of the two circular (or ellipsoidal) patterns resulting from a plane cross-section of the real structure;  $W$ , the maximum width of the toroidal structure and;  $Z_l$  and  $Z_r$ , the above source height of the structures.

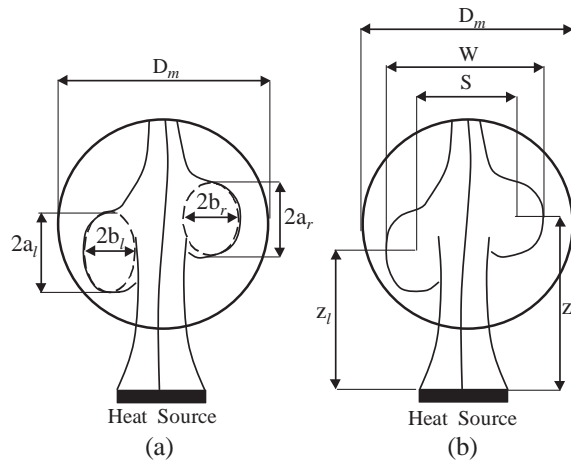


Fig. 6. Scheme of the relevant dimensions of vertical structures.

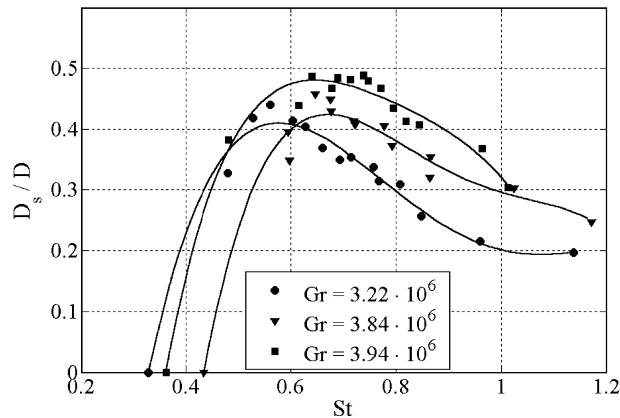


Fig. 7. Evolution of the vortical structure diameter as a function of the Strouhal number.

Similar tendencies were observed for the three test temperatures. Indeed,  $S$ ,  $W$ , and  $D_S$  all reach a maximum. This maximum was obtained for  $f=1.6$  Hz,  $f=2.2$  Hz, and  $f=2.6$  Hz for  $T_0=100$ , 150, and 200 °C, respectively. The maximum of  $W$  for the observed structures ranged between 7.5 cm and 8.5 cm. It was thus of the order of magnitude of the diameter of the heat source. This is in good agreement with other research works [1,2,6,7]. To further illustrate this,  $D_S/D$  has been plotted for each temperature as a function of the Strouhal number  $St$  based on the mean advection velocity and the excitation frequency  $f$  (see Fig. 7). Temperatures are expressed in terms of the global Grashof number  $Gr$ . Assuming that  $D_S$  is maximum when the excitation frequency coincides with the flow preferential mode, the results tend to indicate that the source temperature or the Grashof number is an influencing parameter. Moreover, the higher the source temperature is, the larger the structures are for a given excitation frequency greater than the preferential mode. The contrary is observed for  $f$  smaller than this natural frequency. Although not many cases were investigated with respect to the source temperature, the critical Strouhal number  $St_c$ , which corresponds to the flow preferential mode, tends to increase with the Grashof number although it seems to reach an asymptote at  $St=0.64$ . Note finally that the experiments reported here have allowed characterizing only one instability mode for each test configuration. Ongoing experiments based on another technique, namely ultrasound scattering, have allowed detecting at least two instability modes in experimental test conditions identical to the ones described here. The existence of additional instability modes would reflect a filtering frequencies capacity of thermal plumes.

## 5. Conclusions

Flow visualizations were performed with the Schlieren technique to characterize instabilities in an initially laminar axisymmetric thermal plume subjected to controlled symmetrical disturbances of varicose mode. For the present test configuration, flow laminarity was preserved for source temperatures up to 200 °C in the absence of any excitation.

Instabilities developed only for excitation frequencies ranging between  $f=1$  Hz and  $f=9$  Hz. In this case, structures formed at a rate that coincided with the excitation frequency or, at least, that was in phase with it. This result is in good agreement with earlier results.

The size of the developing instabilities was maximum in the case where the excitation frequency corresponded to the plume preferential mode ( $1.6 \text{ Hz} < f < 2.6 \text{ Hz}$ ). These maxima were of the order of magnitude of the heat source diameter. They ranged between 7.5 cm and 8.5 cm, increasing with increasing the flow natural frequency, which in turn was found to increase with the heat source temperature. The existence of preferential modes of instability provides further evidence of the filtering capacity of thermal plumes.

### Nomenclature

$D$	Diameter of the disk-heated source, m
$D_e$	Equivalent diameter of vortical structures section defined in Eq. (3), m
$D_m$	Diameter of the mirror, m
$D_S$	Mean diameter of vortical structure section, m
$f$	Frequency, Hz
$g$	$9.81, \text{ m/s}^2$
$Gr$	Grashof number ( $=g\beta(T_0 - T_\infty)D^3/\nu^2$ )
$n$	Index of refraction of the fluid transparent medium (Eq. (1))
$Ri$	Richardson number of a free jet ( $=\rho_\infty - \rho_0)gw]/\rho_\infty U_0^2$ )
$U_a$	Mean advection velocity of vortical structures defined in Eq. (3), m/s
$U_0$	Mean velocity of a free jet at the origin, m/s
$S$	Separation between the centers of a vortical structure in cross section, m
$St$	Strouhal number ( $=fD/U_a$ )
$t$	Time, s
$T$	Temperature (Eq. (2)), K
$T_0$	Temperature of the heated disk, K
$T_\infty$	Temperature of the quiescent fluid medium, K
$w$	Slot width of a two-dimensional jet, m
$W$	Maximum wide of vortical structure, m
$x$	Coordinate in normal direction with respect to light beams (Eq. (2)), m
$y$	Coordinate in the direction of light beam (Eq. (2)), m
$z$	Axial cylindrical coordinate for axisymmetric flows, m

### Greek symbols

$\beta$	Volumetric coefficient of thermal expansion, $1/\text{K}$
$\nu$	Kinematic fluid viscosity, $\text{m}^2/\text{s}$
$\rho$	Density of the fluid flow (Eqs. (1) and (2)), $\text{kg}/\text{m}^3$
$\rho_0$	Density of the fluid flow at the origin, $\text{kg}/\text{m}^3$
$\rho_\infty$	Density of the fluid flow at the quiescent medium, $\text{kg}/\text{m}^3$

### Acknowledgements

The study reported in this paper was supported by CONICYT under grants Fondecyt No. 1010135 and No. 7010135. We gratefully acknowledge valuable scientific, technical, and material support of Dr. Christophe Baudet.

**References**

- [1] B.M. Cetegen, Y. Dong, M.C. Soteriou, *Phys. Fluids* 10 (7) (1998) 1658.
- [2] B.M. Cetegen, *Fire Saf. J.* 31 (1998) 299.
- [3] B. Gebhart, Y. Jaluria, R. Mahajan, B. Sammakia, *Buoyancy-induced flows and transport*, Textbook edition, Hemisphere Publishing Corporation, New York, 1988.
- [4] L. Pera, B. Gebhart, *Int. J. Heat Mass Transfer* 14 (1971) 975.
- [5] R.G. Bill, B. Gebhart, *Int. J. Heat Mass Transfer* 18 (1975) 513.
- [6] S. Kimura, A. Bejan, *Int. J. Heat Mass Transfer* 26 (1983) 1515.
- [7] B.M. Cetegen, *Phys. Fluids* 9 (12) (1997) 3742.
- [8] G. Tanda, *Opt. Methods Heat Mass Transf.* 1 (1999) (Homepage).
- [9] G.S. Settles, *Schlieren and Shadowgraph Techniques*, Textbook edition, Springer-Verlag, Berlin, 2001.
- [10] J.C. Elicer-Cortés, R. Contreras, D. Boyer, M. Pavageau, R.H. Hernández, *Exp. Therm. Fluid Sci.* 28 (2004) 803.
- [11] B. Han, R.J. Goldstein, *Int. J. Heat Mass Transfer* 46 (2003) 3975.